

ACETIC ACID ENHANCED PURIFICATION OF CRUDE CELLULOSE FROM SUGARCANE BAGASSE: STRUCTURAL AND MORPHOLOGICAL CHARACTERIZATION

Jing Bian,^a Feng Peng,^{a,b} Xiao-Peng Peng,^{c,d} Pai Peng,^b Feng Xu,^a and Run-Cang Sun^{a,b,*}

Crude cellulose prepared from alkali-extracted sugarcane bagasse was subjected to a rapid purification treatment with a mixture of 80% acetic acid-68% nitric acid (10/1, v/v) at 120 °C for 15 min. The yields of the preparations decreased slightly from 57.3%-58.6% in the crude cellulose preparations to 50.3%-51.9% in the purified cellulose samples. The purification treatment removed large amounts of resistant hemicelluloses strongly associated to the cellulose. XRD analysis revealed that the structure of both the crude and purified cellulose was cellulose I. Compared to the crude cellulose, a slight increase in the crystallinity index of the purified cellulose was observed by FTIR, XRD, and CP/MAS ¹³C NMR analyses. In addition, SEM showed that the microfibril surface of the crude cellulose was almost free of trenches, but many terraces, steps, and kinks formed in the preparations after the purification.

Keywords: Sugarcane bagasse; Cellulose; Acetic acid-nitric acid; Crystallinity

Contact information: a: Institute of Biomass Chemistry and Technology, Beijing Forestry University, Beijing 100083, China; b: State Key Laboratory of Pulp and Paper Engineering, South China University of Technology, Guangzhou 510640, China; c: Chinese Academy of Forestry, Beijing 100091, China; d: College of Biological Sciences and Biotechnology, Beijing Forestry University, Beijing 100083, China; *Corresponding author: rcsun3@bjfu.edu.cn

INTRODUCTION

Cellulose is the most abundant naturally occurring organic polymer, representing about 1.5×10^{12} tons of the world's total annual biomass production, and is considered an almost inexhaustible source of raw material (Klemm *et al.* 2005). Cellulose and its derivatives are used in a diverse array of applications, such as fibers, films, plastics, coatings, suspension agents, composites, toothpastes, flow enhancers, drilling fluids, shampoos, foodstuffs, and so forth, due to their availability, biocompatibility, biological degradability, and sustainable production (Kadla and Gilbert 2000). The physical, chemical, or enzymatic transformation and the conception of new material are closely related to the properties and structure of cellulose. Therefore, extensive effort has been devoted to chemical and structural studies on cellulose.

Cellulose is a linear homopolymer of (1 → 4)-linked β-D-glucopyranose units (Glc), aggregated to form a highly ordered structure (Oh *et al.* 2005), which is composed of both crystalline and amorphous parts. To be more specific, cellulose has a flat, ribbon-like conformation. The repeat unit is comprised of two anhydroglucose rings linked together through oxygen covalently bonded to C-1 of one glucose ring and C-4 of the adjoining ring. (Samir *et al.* 2005). A distinct number of glucan chains ((C₆H₁₀O₅)_n;

$n = 10,000$ to $15,000$, where n is dependent on the cellulose source material) assemble during biosynthesis, forming microfibrils, then fibres, and higher cellulose organization structures (Brown 1996). The β -linkages in cellulose are highly stable and resistant to chemical attack because of the high degree of intra- and inter-molecular hydrogen bonding. In addition, there are six polymorphs of cellulose (I, II, III_I, III_{II}, IV_I, and IV_{II}), which can be interconverted (O'Sullivan 1997). Cellulose I, also termed native cellulose, is the most abundant and the only form found in nature. It is a composite of two distinct crystalline phases, namely cellulose I _{α} and I _{β} . Electron diffraction studies have revealed that cellulose I _{α} can be considered an allomorph, having a 1-chain triclinic unit cell, and that I _{β} can be considered another allomorph, having a 2-chain monoclinic unit (Sugiyama *et al.* 1991), but they differ in hydrogen bonding. The crystal structure of cellulose in higher plants, such as wood and cotton, is that of cellulose I _{β} , while cellulose I _{α} is reported as the dominant polymorph in bacterial and algal cellulose (Nishiyama *et al.* 2002). Cellulose I _{α} is metastable and can be converted to the more stable form I _{β} by hydrothermal treatments (Debzi *et al.* 1991). Noncrystalline cellulose forms are also present in the fibril, which are a mixture of paracrystalline cellulose and cellulose at inaccessible and accessible fibril surfaces (Duchesne *et al.* 2001).

In lignocellulosic material, cellulose is bonded together with hemicelluloses and lignin by covalent bonding, various intermolecular bridges, and van der Waals forces, forming a complex structure (Kumar *et al.* 2010). Sasaki and Taylor (1984) discussed the effect of the hemicellulose xyloglucan binding to the fibrils and found that the binding of xyloglucan could be a regulator of cellulose fibrillar size. It has also been reported that the strong association between hemicelluloses and cellulose fibrils is believed to decrease the average crystallinity of the cellulose fibrils (Whitney *et al.* 1998). Because of the complexity of the cell wall structures, it is difficult to isolate pure cellulose from lignocellulosic material. The combination of the chemical and mechanical treatments for wood and plants involves the complete removal of matrix material (mainly hemicelluloses and lignin) to obtain relatively pure cellulose. Likewise, if the removal of the matrix materials is incomplete (*e.g.*, hemicelluloses are only partially removed), the matrix materials can inhibit the coalescence of the microfibril bundles during drying and facilitate the subsequent fibrillation of the material (Iwamoto *et al.* 2008). In this study, a rapid and simple protocol for crude cellulose purification is described and the structure and morphology of the crude and purified cellulose obtained is studied. The changes between these different cellulose samples were investigated using wide-angle X-ray diffraction (XRD), Fourier transform infrared (FTIR), scanning electron microscopy (SEM), and solid polarized/magic angle spinning (CP/MAS) ¹³C NMR spectroscopy. The yield, intrinsic viscosity, and molecular weight of all cellulose were also determined.

EXPERIMENTAL

Materials

Sugarcane bagasse was collected in a sugar factory (Guangzhou, China). It was air dried, milled, and screened to select the fraction of particles that passed through a 40-mesh screen and was retained on an 80-mesh screen. Then, the powder was homogenized

in a single lot and stored until needed. All standard chemicals were analytical grade, purchased from Sigma Chemical Company (Beijing).

Isolation and Purification of Cellulose

The dried sugarcane bagasse powder was first delignified with sodium chlorite in acidic solution (pH 3.8 to 4.0, adjusted by acetic acid) at 75 °C for 2 h. After treatment, the residue (holocellulose) was filtered off, washed thoroughly with distilled water, and further dried in a cabinet oven with air circulation. The holocellulose was then extracted with 10% KOH with a solid-to-liquor ratio of 1:20 (g mL⁻¹) for 10 h at 20, 25, 30, 35, 40, 45, and 50 °C. The residue that was rich in cellulose was filtrated off and washed thoroughly with water until the filtrate was neutral, and dried in an oven at 55 °C for 16 h. These preparations were labeled CC20, CC25, CC30, CC35, CC40, CC45, and CC50, respectively. To obtain purified cellulose, these crude cellulose preparations (~0.5 g) were individually measured into Pyrex tubes and 10.0 mL of 80% (v/v) acetic acid and 1.0 mL of 68% nitric acid were added. Subsequently, the tubes were sealed using screw-caps fitted with Teflon liners and immersed in a pre-heated oil bath, where the temperature was kept at 120 °C for 15 min. After cooling, the solid was separated from the liquid phase by filtration and washed sequentially with 95% ethanol, distilled water, and 95% ethanol to remove traces of nitric acid and extraction breakdown products. The purified cellulose preparations obtained from the corresponding crude cellulose samples were considered to be PC20, PC25, PC30, PC35, PC40, PC45, and PC50, respectively. To reduce errors and confirm the results, each experiment in this study was conducted in duplicate, and the average values were calculated under the same conditions.

Characterization of Crude and Purified Cellulose

Viscosity of the crude and purified cellulose was determined by the cupri-ethylene-diamine (CED) method (Wang *et al.* 2009). The viscosity average DP (degree of polymerization) (P) of the cellulose samples was estimated from their intrinsic viscosity $[\eta]$ in CED hydroxide (cuene) solution.

$$P^{0.90} = 1.65 [\eta]/\text{mL g}^{-1} \quad (1)$$

The molecular weight of the cellulose was then calculated, using P multiplied by 162, the molecular weight of an anhydroglucose.

High performance anion exchange chromatography (HPAEC) coupled with a pulsed amperometric detector was used to analyze the typical compositions of both the crude and purified cellulose. The sample (5 mg) was treated with 72% H₂SO₄ (0.125 mL) for 45 min at room temperature. Then the reaction mixture was diluted to 10% H₂SO₄ and heated at 105 °C for 2 h. After hydrolysis, the sample was diluted 50-fold, filtered, and separated in a 5 mM NaOH isocratic eluent (carbonate-free and purged with nitrogen) for 20 min, followed by a 0 to 75 mM NaAc gradient in 5 mM NaOH for 15 min. Then, the columns were washed with 200 mM NaOH to remove carbonate for 10 min, followed by an elution with 5 mM NaOH for 5 min to re-equilibrate the column before the next injection. The total analysis time was 50 min, and the flow rate was 0.4 mL/min.

Calibration was performed with standard solutions of L-arabinose, D-glucose, D-xylose, D-mannose, D-galactose, glucuronic acid, and galacturonic acids.

The crystallinities of the crude and purified cellulose were measured using an XRD-6000 instrument (Shimadzu, Japan) with a Cu K α radiation source ($\lambda = 0.154$ nm) at 40 KV and 30 mA. Samples were scanned at a speed of 2°/min, ranging from $2\theta = 5^\circ$ to 50° . The crystallinity, as expressed by the crystallinity index (*CrI*), was determined by the Segal method (1959), using the height of the 200 peak (I_{200} , $2\theta = 22.7^\circ$) and the minimum between the 200 and 110 peaks (I_{am} , $2\theta = 18^\circ$) by the following equation:

$$CrI = 100 \times [(I_{200} - I_{am})/I_{200}] \quad (2)$$

The expression requires that the amorphous material diffracts with the same intensity at 18° and 22.7° and that the crystalline cellulose does not contribute to the intensity at 18° (Thygesen *et al.* 2005).

FTIR spectra were recorded using a Nicolet iN10 FTIR microscope (Thermo Nicolet Corporation, Madison, WI), equipped with a liquid nitrogen-cooled MCT detector. Each sample was placed onto a micro-compression cell made of diamond and pressed in order to squeeze it. The squeezed cellulose samples can be analyzed with the diamond anvil cell, placing them directly on the stage of FTIR microscope. The spectra collected were the average of 64 scans recorded at a resolution of 8 cm^{-1} in the range of 4000 to 750 cm^{-1} .

CP/MAS ^{13}C NMR spectra of the samples were obtained at 100 MHz using a Bruker AV-III 400 M spectrometer (Germany). Samples were packed in 4 mm zirconia (ZrO_2) rotors, and the measurements were performed using a CP pulse program with 1 ms match time and a 2 s delay between transients. The spinning rate was 5 kHz. Calibration was done externally to the carbonyl carbon of glycine at 176 ppm.

Scanning electron microscopy of the crude and purified cellulose samples was carried out with a Hitachi S-3400N II (Hitachi, Japan) instrument at 15 KV. Before the determination, samples were mounted with conductive glue and coated with a thin layer of gold to improve the conductivity and thus the quality of the SEM images.

RESULTS AND DISCUSSION

Yield, Intrinsic Viscosity (η), DP, and M_w of Crude and Purified Cellulose

Many attempts have been made to isolate cellulose from various biomass sources, in which aqueous alkali extraction is the most efficient method for removing large amounts of hemicelluloses from the original or delignified lignocelluloses. Hydroxyl ions can cause swelling of cellulose and disruption of the intermolecular hydrogen bonds between cellulose and hemicelluloses, substantially solubilizing hemicelluloses into aqueous solution, and resulting in solid residue enriched with cellulose. In this study, acidified sodium chlorite was applied to delignify the sugarcane bagasse material as an initial step. Hemicelluloses were removed by alkali extraction with 10% KOH for 10 h at different temperatures to obtain seven crude cellulose samples. Subsequently, the extraction with acetic acid-nitric acid mixture (80% acetic acid-68% nitric acid, 10/1, v/v)

was carried out at 120 °C for 15 min to prepare the purified cellulose. The yields of the crude and purified cellulosic preparations are listed in Table 1. As can be seen, the yields of crude cellulose (CC20, CC25, CC30, CC35, CC40, CC45, and CC50) ranged between 57.3% and 58.6%, based on the original holocellulose. This indicated that the temperature used (20 °C to 50 °C) did not affect the yield of crude cellulose. Additionally, in comparison with the yield of crude cellulose, the yields of corresponding purified cellulose slightly decreased to 50.3%-51.9%. The decreased yields were ascribed to the fact that large amounts of the residual hemicelluloses were removed by the acetic acid-nitric acid medium under the conditions given.

Table 1. Yield of Crude and Purified Cellulose (% Dry Matter of the Initial Amount of Delignified Material)

	Cellulose samples						
	20	25	30	35	40	45	50
Crude cellulose (CC)*	58.1	57.4	58.6	57.3	57.9	58.1	57.6
Purified cellulose (PC)**	51.2	50.9	51.2	50.3	50.8	51.9	51.6

* Represents the crude cellulose samples isolated with 10% KOH at 20 °C, 25 °C, 30 °C, 35 °C, 40 °C, 45 °C, and 50 °C. ** Represents the corresponding crude cellulose samples treated with 80% acetic acid-68% nitric acid (10:1, v/v) at 120 °C for 15 min.

The viscosity average degree of polymerization of all cellulose samples was estimated from their intrinsic viscosity in CED hydroxide (cuene) solution. Table 2 gives the intrinsic viscosity (η), viscosity average DP (P), and molecular weight (M_w) of the crude and purified cellulose. Apparently, the treatment with acetic acid-nitric acid mixture led to a decrease in intrinsic viscosity from >970 to ~190 mL g⁻¹. This suggested that the treatment with a mixture of acetic and nitric acids resulted in a degradation of cellulose macromolecules. It has been reported that during treatment with an acetic acid-nitric acid medium, nitric acid is degraded into nitrogen dioxide, oxygen, and water at a relatively high temperature ($2\text{HNO}_3 \rightarrow 2\text{NO}_2 + \text{O} + \text{H}_2\text{O}$) (Sun *et al.* 2004). The various substitutions, side chains cleavage, and oxidation reactions are observed with nitric acid. In that case, lignin and hemicelluloses are degraded or oxidized. However, from this study, it was found that the system used can also react with the cellulose under higher temperatures, although it is more reactive towards lignin than cellulose.

Table 2. Intrinsic Viscosity (η), the Viscosity Average DP (P), and Molecular Weight (M_w) of the Crude and Purified Cellulose Samples

	Crude cellulose samples *							Purified cellulose samples*						
	CC20	CC25	CC30	CC35	CC40	CC45	CC50	PC20	PC25	PC30	PC35	PC40	PC45	PC50
η	314.5	329.2	327.5	325.6	301.4	297.0	296.7	66.4	68.3	69.2	69.8	70.5	69.7	69.1
P	1039.3	1093.6	1087.3	1080.2	991.4	975.2	974.1	184.6	190.5	193.3	195.2	197.3	194.8	193.0
M_w	168370	177160	176140	174990	160610	157980	157800	29910	30860	31310	31620	31960	31560	31270

* Corresponding to the cellulose samples in Table 1

Compositional Analysis

The results of neutral sugar composition of the crude and purified cellulose preparations are given in Table 3. Apparently, glucose is the predominant neutral sugar component, comprising 80.0% to 83.3% of the total sugars in the crude cellulose samples. A substantial amount of xylose (13.3% to 17.8%) and minor quantities of arabinose (0.8% to 1.3%), galactose (0.1% to 0.3%), and uronic acids (1.3% to 2.3%) were also detected in the crude cellulose samples. Hemicelluloses are integrated into the structure of cellulose and located within and between cellulose fibrils (Duchesne *et al.* 2001). The current data implied that alkali treatment cannot extract all the hemicelluloses and only solubilized large proportions of the hemicelluloses into the solution from the delignified material. The solid phase (crude cellulose) still contained a noticeable amount of hemicelluloses, which may be the relatively resistant part of hemicelluloses in the sample. A further treatment of the crude cellulose with 80% acetic acid-68% nitric acid at 120 °C for 15 min removed most of the residual hemicelluloses. The purified cellulose contained only minor quantities of xylose sugars (7.1% to 8.5%), indicating a much higher purity compared to the corresponding crude cellulose preparations. This phenomenon revealed that, under the conditions given, the acetic acid-nitric acid medium could remove large quantities of the resistant hemicelluloses strongly bound to the cellulose.

Table 3. Content of Neutral Sugars and Uronic Acids of the Crude and Purified Cellulose Samples

Sugars (%)	Crude cellulose samples*							Purified cellulose samples*						
	CC20	CC25	CC30	CC35	CC40	CC45	CC50	PC20	PC25	PC30	PC35	PC40	PC45	PC50
Ara**	1.3	1.0	1.0	1.0	0.9	1.0	0.8							
Gal**	0.3	0.2	0.2	0.2	0.2	0.2	0.1							
Glc**	83.3	83.1	82.2	80.6	81.3	80.1	80.0	92.1	92.3	92.9	91.5	92.5	92.1	91.8
Xyl**	13.3	13.5	14.7	16.7	16.2	17.0	17.8	7.9	7.7	7.1	8.5	7.5	7.9	8.2
GlcA**	0.2	0.2	0.2	0.1	0.2	0.1	0.1							
GalA**	1.5	2.1	1.7	1.4	1.2	1.7	1.2							

* Corresponding to the cellulose samples in Table 1; ** Ara, arabinose; Gal, galactose; Glc, glucose; Xyl, xylose; GlcA, glucuronic acid; GalA, galacturonic acid

X-ray diffraction has been widely used to evaluate the crystalline structure of cellulose, since it provides a qualitative and semi-quantitative evaluation of the amorphous and crystalline cellulosic components in a sample (Park *et al.* 2010). The XRD peak height method, which involves measurement of just two heights in the X-ray diffractogram, is easy to use for comparing the relative differences between samples. In this study, the crystal features of the purified cellulose PC20, PC35, and PC50 and the corresponding crude cellulose CC20, CC35, and CC50 were determined using this method (Fig. 1).

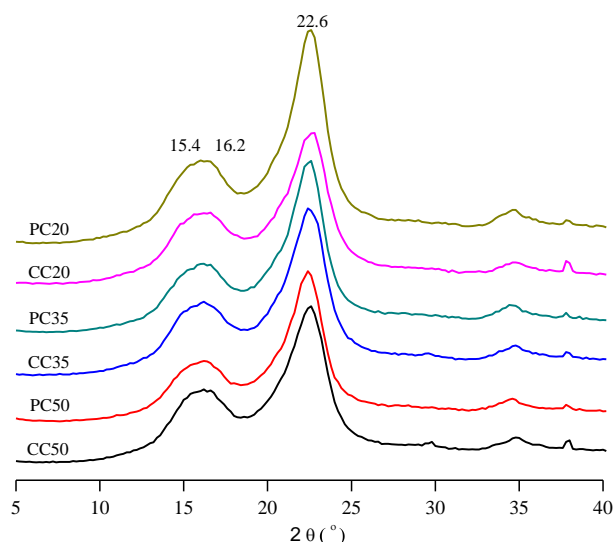


Fig. 1. XRD patterns of the crude cellulose samples CC20, CC35, CC50, and the purified cellulose preparations PC20, PC35, and PC50

X-ray Diffraction

It can be seen that all of the cellulose samples had similar diffraction peaks around 15.4° , 16.2° , and 22.7° as is the typical diffraction pattern of cellulose I. Further evidence of the cellulose I structure is that there was no doublet in the intensity of the main peak at 22° (Morán *et al.* 2008). The peaks at $2\theta = 15.4^\circ$ and 16.2° are the overlapping of $1\bar{1}0$ and 110 reflections (Zuluaga *et al.* 2009). In addition, the crystallinity index was calculated as mentioned above and is given in Table 4. A slight increase in the crystallinity index was observed from 66.0, 67.7, and 66.8 for CC20, CC35, and CC50 to 73.2, 72.4, and 71.5 for PC20, PC35, and PC50, respectively. This was probably due to the fact that the treatment using 80% acetic acid-68% nitric acid (10:1, v/v) reduced the content of the residual hemicelluloses or even a small amount of amorphous cellulose. When hemicellulose and amorphous cellulose were removed or degraded during the treatment, the fiber surface became more open and porous with well-defined fibril aggregates. However, both porous and compact regions may be seen adjacent to each other, causing the increase in the crystallinity index (Duchesne and Daniel 2000). It should be noted that the XRD height method produces values that are significantly higher than other methods and it could not be used to estimate the exact amount of crystalline and amorphous structures in a cellulose sample.

Table 4. Crystallinity Indices of the Crude and Purified Cellulose Samples

Cellulose samples*	XRD	FTIR		C-4 NMR
		$\alpha 1427 \text{ cm}^{-1}/\alpha 899 \text{ cm}^{-1}$	$\alpha 1369 \text{ cm}^{-1}/\alpha 2901 \text{ cm}^{-1}$	
CC20	66.0	1.59	0.26	43.6
CC35	67.7	2.02	0.37	41.5
CC50	66.8	2.36	0.37	41.9
PC20	73.2	4.65	0.34	49.9
PC35	72.4	4.06	0.65	50.6
PC50	71.5	4.54	0.68	48.9

* Corresponding to the cellulose samples in Table 1

FTIR Spectra

FTIR spectroscopy was conducted to compare the molecular conformational changes of the crude and purified cellulose. Figure 2a shows the FTIR spectra of the crude cellulose preparations CC20, CC35, and CC50. All the spectra displayed common characteristics of cellulose: the sharp band at 3348 cm^{-1} is assigned to hydroxyl group (O-H), and the peak at 2929 cm^{-1} indicates the C-H stretching in CH_2 and CH_3 groups (Fengel 1993). The absorption at 1632 cm^{-1} is due to bending of the absorbed water. The most important bands that help to identify the cellulose component are: 1420 cm^{-1} , attributed to amorphous cellulose and crystallized cellulose II and 1430 cm^{-1} , attributed to amorphous cellulose and crystallized cellulose I (Colom and Carrillo 2005). The spectra obtained in this study show the band at 1427 cm^{-1} , which suggests that the samples contained a mixture of crystallized cellulose I and amorphous cellulose, in good agreement with the results of XRD. The doublet at 1335 and 1315 cm^{-1} , which mainly appears in the cellulose of crystalline cellulose I, was observed and can be assigned to C-OH plane bending and CH_2 wagging, respectively (Garside and Wyeth 2004). The OH plane deformation also exhibits a signal at 1200 cm^{-1} . The band at 1161 cm^{-1} originated from C-O antisymmetric bridge stretching and the signal at 1057 cm^{-1} is from C-O-C pyranose ring skeletal vibration. A small sharp band at 899 cm^{-1} is indicative of β -glycosidic linkages between glucose in cellulose.

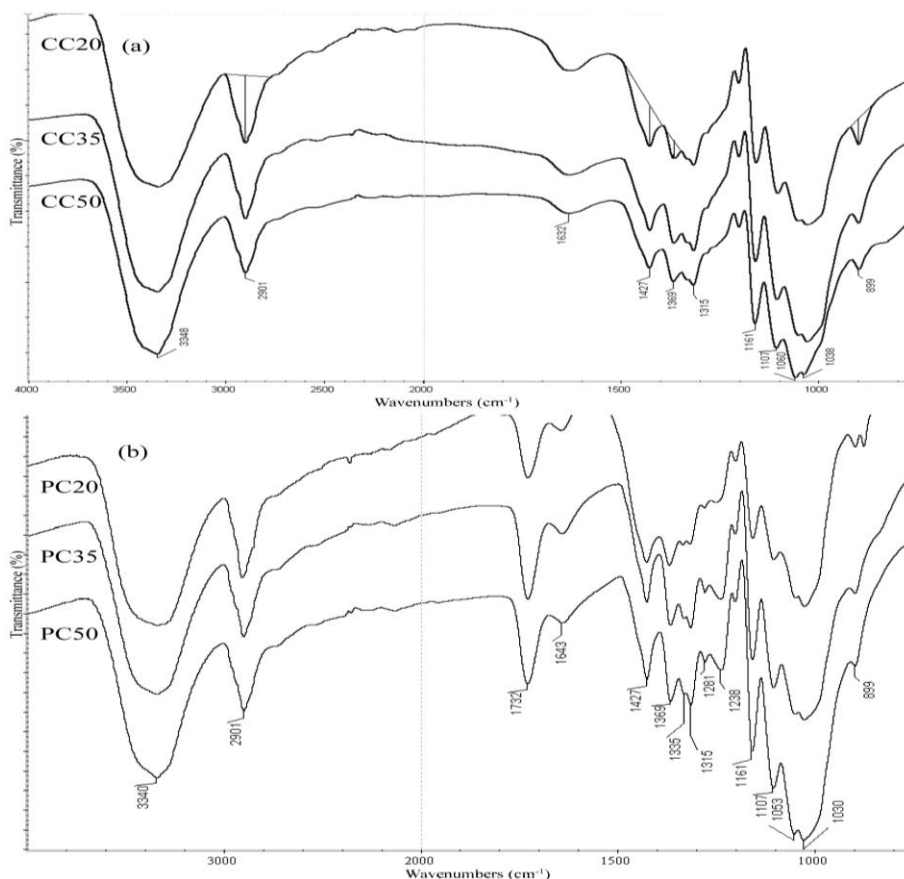


Fig. 2. FTIR spectra of the crude cellulose samples CC20, CC35, CC50 and the purified cellulose samples PC20, PC35, and PC50

Figure 2b shows the structural changes of the purified cellulosic samples PC20, PC35, and PC50. In contrast to the spectra of the corresponding crude cellulose, the spectra of the purified cellulose show an intensive ester band at 1732 cm^{-1} (C=O ester), indicating the occurrence of acetylation during the acetic acid-nitric acid treatment. The band at 1238 cm^{-1} , assigned to C-O of acetyl, is also characteristic of acetylated polysaccharide (Adebajo and Frost 2004). This suggested that the treatment with a mixture of acetic and nitric acids did lead to a noticeable acetylation reaction.

In addition, the infrared absorption ratios of $\alpha_{1429\text{ cm}^{-1}}/\alpha_{893\text{ cm}^{-1}}$ and $\alpha_{1372\text{ cm}^{-1}}/\alpha_{2900\text{ cm}^{-1}}$ have been proposed for measuring the crystallinity in cellulosic material (Nelson and O'Connor 1964). The crystallinity of the six cellulose samples was calculated, and results are listed in Table 4. The data were in agreement with the results from XRD analysis, further confirming the decrease of cellulose crystallinity after purification.

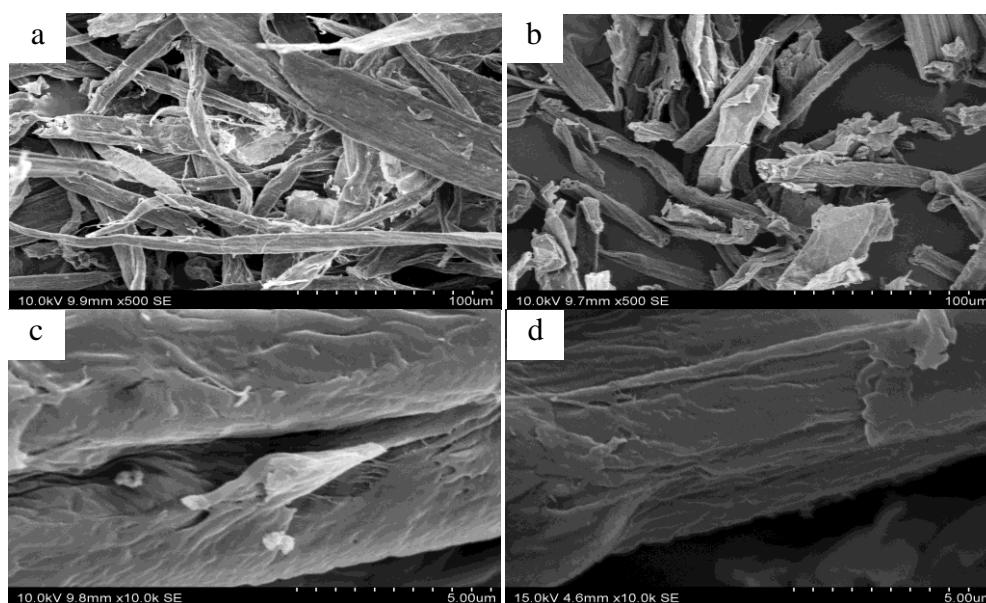


Fig. 3. SEM images at various magnifications of crude cellulose CC50 and purified cellulose PC50. (a) CC50 at 500 \times (b) PC50 at 500 \times (c) CC50 at 10000 \times (d) PC50 at 10000 \times

Scanning Electron Microscopy Images

Scanning electron microscopy has been an important tool that has been extensively employed for morphological inspection. Figure 3 shows the SEM micrographics of the crude cellulose CC50 (Fig. 3a, Fig. 3c) and purified cellulose PC50 (Fig. 3b, Fig. 3d) under various magnifications. Figure 3a clearly shows the shape of the well-separated macrofibrils. A closer look at the macrofibril surface at a higher magnification (Fig. 3c, 10000 \times) shows that the surface of crude cellulose is almost free of trenches, but there are obvious boundary edges in different regions. Figure 3b shows that the macrofibrils of the purified cellulose PC50 are still well separated, but the lengths of the macrofibrils dropped. The SEM image (Fig. 3d, 10000 \times) of one individual macrofibril at higher magnification shows that many terraces, steps, and kinks formed after the purification treatment. The changes of the morphology may be explained as follows. Hemicelluloses play the role of regulator during the association of cellulose chains, and influence the pattern of aggregation of cellulose into fibril and fibril aggregates during the biogenesis

of the cell wall in higher plants (Tokoh *et al.* 1998). It has been suggested that hemicelluloses are intimately integrated into the structure of the cellulose and locate within and between the cellulose fibrils (Duchesne *et al.* 2001). Consequently, when a large amount of the resistant hemicelluloses strongly associated to the cellulose were removed during the acetic acid treatment, the intact and smooth surface of the microfibril changed, and it showed many terraces, steps, and kinks. The same phenomenon has also been observed by Zhao *et al.* (2007), who ascribed the changes to the removal of reactive amorphous cellulose. In the present study, the purification treatment could also remove a small amount of amorphous cellulose. Therefore, we propose that the changes of the morphology are due to the removal of hemicelluloses and a small amount of amorphous cellulose.

CP/MAS ^{13}C NMR Spectra

CP/MAS involves cross polarization to enhance the ^{13}C signal, high power proton dipolar decoupling to eliminate dipolar line-broadening due to protons, and spinning of the sample about an axis at a particular angle to the static field to eliminate chemical shift anisotropy (Atalla and Vanderhart 1984). Therefore, solid-state CP/MAS ^{13}C NMR spectroscopy provides an accurate measure of the crystallinity of the cellulose sample. The CP/MAS ^{13}C solid-state spectra of cellulose PC20, CC20, PC35, CC35, PC50, and CC50 are shown in Fig. 4.

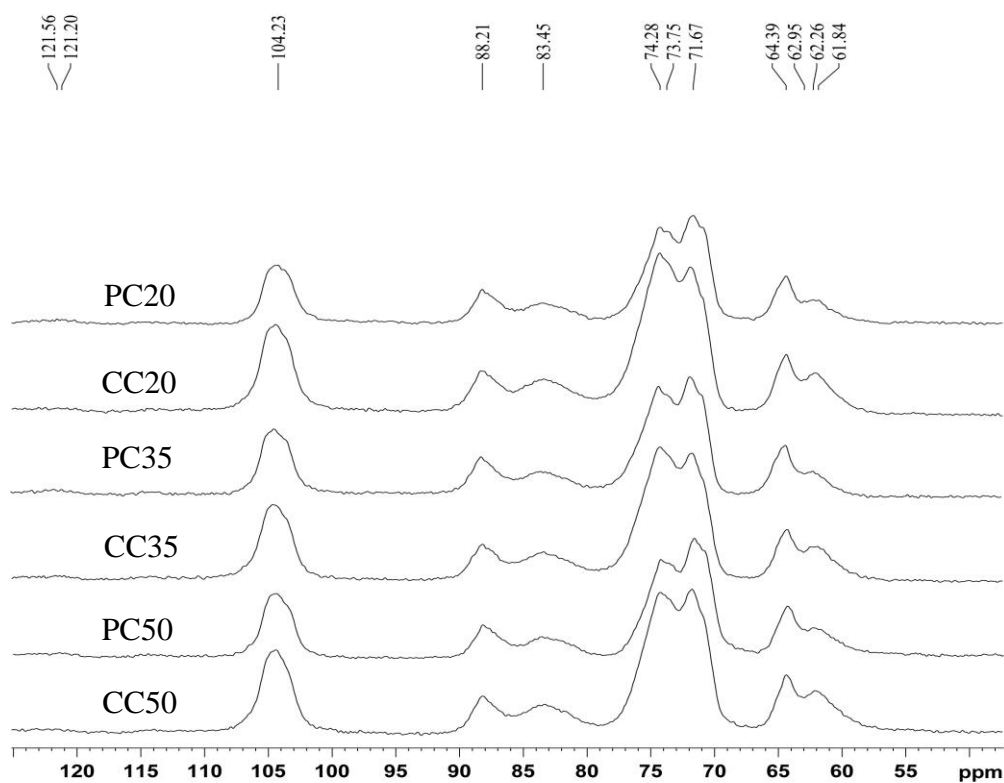


Fig. 4. CP/MAS ^{13}C NMR spectra of the crude cellulose samples CC20, CC35, CC50 and the purified cellulose samples PC20, PC35, and PC50

The most informative region in the NMR spectra is the signal cluster between 80 and 92 ppm originating from the C-4 region. This region contains sharp signals between 86 and 92 ppm corresponding to C-4 carbons from the crystalline, as well as paracrystalline regions. The signals of C-4 carbons in more disordered regions are distributed in a broader band, ranging from 80 to 86 ppm. More precisely, line shape analysis based on a nonlinear least squares fitting analysis has been performed on this area, and it was found that the signals at 80 to 86 ppm are attributable to C-4 carbons at the accessible fibril surface and inaccessible fibril surface (Larsson *et al.* 1999). In addition, the ratio of the area in the 86 to 92 ppm region to the total peak area in these two regions is designated as the crystallinity index (Sannigrahi *et al.* 2008).

As can be seen in Table 4, the crystallinity index using this NMR C-4 peak calculation method was 43.6% for CC20, 41.5% for CC35, and 41.9% for CC50. After the purification treatment, the crystallinity index of the corresponding cellulose increased to 49.9%, 50.6%, and 48.9%, respectively. This suggested that the presence of the residual hemicelluloses tended to reduce the crystallinity index, since these components contribute to the signal intensity in the amorphous or less ordered regions of the CP/MAS spectra (Sannigrahi *et al.* 2008). The NMR C-4 peak calculation produces a lower crystallinity index than the XRD peak height method. Although these methods give different crystallinity index results for the given cellulose, the order of crystallinity for these cellulose samples is relatively consistent within both measurement techniques. This is consistent with the conclusion of Park *et al.* (2010), who tested eight cellulose samples with different methods and found that the XRD peak height method produces a higher value than NMR. Moreover, the 60 to 67 ppm region of the spectra corresponding to C-6 is similar to that of the C-4 in that the spectra include a cluster of sharper resonances and a broader upfield wing. The resonance at 105 ppm is due to C-1, and the features between 69 and 81 ppm are assigned to C-2, C-3, and C-5, collectively. There is no basis for individual assignment.

CONCLUSIONS

1. The treatment with the 80% acetic acid-68% nitric acid system (10:1, v/v) at 120 °C for 15 min can be considered a rapid and simple method for purifying crude cellulose.
2. The protocol removed relatively large quantities of resistant hemicelluloses strongly associated to the cellulose and caused partial degradation of the cellulose macromolecules.
3. The structure of both the crude and purified cellulose was found to be cellulose I.
4. The combination of XRD, FTIR, and ¹³C CP/MAS NMR revealed that the purified cellulose had a higher crystallinity, compared to the corresponding crude cellulose.

ACKNOWLEDGMENTS

The authors are grateful to grants from the Fundamental Research Funds for the Central Universities (BLYJ201215), Natural Science Foundation of China (No. 30930073), the Ministry of Science and Technology (973, 2010CB732204), and the Ministry of Education of China (No. 111).

REFERENCES CITED

- Adebajo, M. O., and Frost, R. L. (2004). "Acetylation of raw cotton for oil spill cleanup application – an FTIR and ^{13}C MAS NMR spectroscopic investigation," *Spectrochim Acta. A* 60(10), 2315-2321.
- Atalla, R. H., and Vanderhart, D. L. (1984). "Native cellulose: A composite of two distinct crystalline forms," *Science* 223(4663), 283-285.
- Brown, R. M., Jr. (1996). "The biosynthesis of cellulose," *J. Macromol. Sci. Part A-Pure Appl. Chem.* 33(10), 1345-1373.
- Colom, X., and Carrillo, F. (2005). "Comparative study of wood samples of the northern area of Catalonia by FTIR," *J. Wood Chem. Technol.* 25(1-2), 1-11.
- Debzi, E. M., Chanzy, H., Sugiyama, J., Tekely, P., and Excoffier, G. (1991). "The Ia \rightarrow I β transformation of highly crystalline cellulose by annealing in various mediums," *Macromolecules* 24(26), 6816-6822.
- Duchesne, I., and Daniel, G. (2000). "Changes in surface ultrastructure of Norway spruce fibres during kraft pulping-visualization by field emission-SEM," *Nord. Pulp Paper Res. J.* 15(1), 54-61.
- Duchesne, I., Hult, E. L., Molin, U., Daniel, G., Iversen, T., and Lennholm, H. (2001). "The influence of hemicellulose on fibril aggregation of kraft pulp fibres as revealed by FE-SEM and CP/MAS ^{13}C -NMR," *Cellulose* 8(2), 103-111.
- Fengel, D. (1993). "Influence of water on the OH valency range in deconvoluted FTIR spectra of cellulose," *Holzforschung* 47(2), 103-108.
- Garside, P., and Wyeth, P. (2004). "Polarised ATR-FTIR characterisation of cellulosic fibres in relation to historic artefacts," *Restaurator* 25(4), 249-259.
- Iwamoto, S., Abe, K., and Yano, H. (2008). "The effect of hemicelluloses on wood pulp nanofibrillation and nanofiber network characteristics," *Biomacromolecules* 9(3), 1022-1026.
- Kadla, J. F., and Gilbert, R. D. (2000). "Cellulose structure: A review," *Cellulose Chem. Technol.* 34(3-4), 197-216.
- Klemm, D., Heublein, B., Fink, H. P., and Bohn, A. (2005). "Cellulose: Fascinating biopolymer and sustainable raw material," *Angew. Chem. Int. Ed.* 44(22), 3358-3393.
- Kumar, S., Gupta, R., Lee, Y. Y., and Gupta, R. B. (2010). "Cellulose pretreatment in subcritical water: Effect of temperature on molecular structure and enzymatic reactivity," *Bioresour. Technol.* 101(4), 1337-1347.
- Larsson, P. T., Hult, E. L., Wickholm, K., Pettersson, E., and Iversen, T. (1999). "CP/MAS ^{13}C -NMR spectroscopy applied to structure and interaction studies on cellulose I," *Solid State Nucl. Mag. Reson.* 15(1), 31-40.

- Morán, J. I., Alvarez, V. A., Cyras, V. P., and Vázquez, A. (2008). "Extraction of cellulose and preparation from sisal fibers," *Cellulose* 15(1), 149-159.
- Nelson, M. L., and O'Connor, R. T. (1964). "Relation of certain infrared bands to cellulose crystallinity and crystal lattice type. Part II. A new infrared ratio for estimation of crystallinity in celluloses I and II," *J. Appl. Polym. Sci.* 8(3), 1325-1341.
- Nishiyama, Y., Langan, P., and Chanzy, H. (2002). "Crystal structure and hydrogen-bonding system in cellulose I β from synchrotron X-ray and neutron fiber diffraction," *J. Am. Chem. Soc.* 124(31), 9074-9082.
- Oh, S. Y., Yoo, D. I., Shin, Y., Kim, H. C., Kim, H. Y., Chung, Y. S., Park, W. H., and Youk, J. H. (2005). "Crystalline structure analysis of cellulose treated with sodium hydroxide and carbon dioxide by means of X-ray diffraction and FTIR spectroscopy," *Carbohydr. Res.* 340(15), 2376-2391.
- O'Sullivan, A. C. (1997). "Cellulose: The structure slowly unravels," *Cellulose* 4(3), 173-207.
- Park, S., Baker, J. O., Himmel, M. E., Parilla, P. A., and Johnson, D. K. (2010). "Cellulose crystallinity index: Measurement techniques and their impact on interpreting cellulase performance," *Biotechnol. Biofuels* 3, 10.
- Samir, M. A. S. A., Alloin, F., and Dufresne, A. (2005). "Review of recent research into cellulosic whiskers, their properties and their application in nanocomposite field," *Biomacromolecules* 6, 612-626.
- Sannigrahi, P., Ragauskas, A. J., and Miller, S. J. (2008). "Effects of two-stage dilute acid pretreatment on the structure and composition of lignin and cellulose in loblolly pine," *Bioenerg. Res.* 1(3-4), 205-214.
- Sasaki, K., and Taylor, I. E. P. (1984). "Specific labelling of cell wall polysaccharides with myo-[2-³H] inositol during germination and growth of *Phaseolus vulgaris L.*," *Plant Cell Physiol.* 25(6), 989-997.
- Segal, L., Creely, J. J., Martin, A. E., and Conrad, C. M. (1959). "An empirical method for estimating the degree of crystallinity of native cellulose using the X-ray diffractometer," *Text. Res. J.* 29(10), 786-794.
- Sugiyama, J., Vuong, R., and Chanzy, H. (1991). "Electron diffraction study on the two crystalline phases occurring in native cellulose from an algal cell wall," *Macromolecules* 24(14), 4168-4175.
- Sun, X. F., Sun, R. C., Su, Y. Q., and Sun, J. X. (2004). "Comparative study of crude and purified celluloses from wheat straw," *J. Agric. Food Chem.* 52(4), 839-947.
- Thygesen, A., Oddershede, J., Lilholt, H., Thomsen, A. B., and Ståhl, K. (2005). "On the determination of crystallinity and cellulose content in plant fibres," *Cellulose* 12(6), 563-576.
- Tokoh, C., Takabe, K., Fujita, M., and Saiki, H. (1998). "Cellulose synthesized by *Acetobacter xylinum* in the presence of acetyl glucomannan," *Cellulose* 5(4), 249-261.
- Wang, K., Jiang J. X., Xu, F., and Sun, R. C. (2009). "Influence of steaming explosion time on the physic-chemical properties of cellulose from Lespedeza stalks (*Lespedeza crytobotrya*)," *Bioresour. Technol.* 100(21), 5288-5294.

- Whitney, S. E. C., Brigham, J. E., Darke, A. H., Reid, J. S. G., and Gidley, M. J. (1998). "Structural aspects of the interaction of mannan-based polysaccharides with bacterial cellulose," *Carbohydr. Res.* 307(3-4), 299-309.
- Zhao, H., Kwak, J., Conradzhang, Z., Brown, H., Arey, B., and Holladay, J. (2007). "Studying cellulose fiber structure by SEM, XRD, NMR and acid hydrolysis," *Carbohydr. Polym.* 68(2), 235-241.
- Zuluaga, R., Putaux, J. L., Cruz, J., Vélez, J., Mondragon, I., and Gañán, P. (2009). "Cellulose microfibrils from banana rachis: Effect of alkaline treatments on structural and morphological features," *Carbohydr. Polym.* 76(1), 51-59.

Article submitted: June 22, 2012; Peer review completed: July 21, 2012; Revised version received and accepted: July 25, 2012; Published: August 8, 2012.